

Photochemistry of Azobenzene in Microporous Aluminophosphate $\text{AlPO}_4\text{-5}$

Zhaohui Lei, Anand Vaidyalingham, and Prabir K. Dutta*

Department of Chemistry, The Ohio State University, 100 West 18th Avenue, Columbus, Ohio 43210

Received: June 12, 1998; In Final Form: August 10, 1998

Photochemical studies of molecules in the organized voids of microporous frameworks is an area of considerable research interest. In this study, we have examined the spectroscopy and photochemistry of *trans*-azobenzene introduced into the 8 Å channels of an aluminophosphate framework, $\text{AlPO}_4\text{-5}$. The acidity of aluminophosphates is considered to be very weak, based on their poor catalytic performance in transformations of organic compounds. However, we report that the Brønsted acidity of the $\text{AlPO}_4\text{-5}$ is enough to protonate the azo groups in azobenzene. This leads to appearance of a band at 418 nm. Also, room temperature emission observed at 518 nm, an unusual spectroscopic feature for azobenzene, is due to the protonated form. Photolysis of the azobenzene/ $\text{AlPO}_4\text{-5}$ sample leads to the formation of benzo[*c*]cinnoline and benzidine. The Lewis acid sites of $\text{AlPO}_4\text{-5}$ are proposed to play an important role in the photocyclization chemistry. Because the number of such acid sites in $\text{AlPO}_4\text{-5}$ is limited, only a fraction of the azobenzene molecules undergo photocyclization. The rest exhibit reversible *cis*–*trans* photoisomerization in the presence of visible and ultraviolet irradiation.

The azobenzene chromophore has elicited considerable interest because of its novel photoisomerization and photocyclization reactions¹ as well as its technological applications in the dye and pigment industry.² The photochemical isomerization around the N=N bond is a classic example of *cis*–*trans* isomerization.³ The mechanism of this isomerization process has been controversial, and two pathways involving either rotation around the N=N bond or inversion through a planar transition state with a sp-hybridized N atom have been proposed.⁴ Both these pathways require an expanded volume in the conversion between the *trans* and *cis* forms, and the dynamics of this isomerization process has provided information on voids in polymer structure.⁵ Incorporation of azobenzene in bilayer assemblies has led to observation of the excitonic state and novel photochemical reactivity and energy transfer.⁶ In these previous studies, the interesting effects arise because the azobenzene moiety is in a constrained environment.

Microporous crystals provide well-defined and controllable voids, and photochemical studies in these matrixes is an area of current interest.^{7a} Controlled chemistry in the microporous cavities may lead to novel electronic and optical materials.^{7b} The recent work of Calzaferri and co-workers in alignment of chromophores within zeolite channels that exhibit energy transfer properties is a good example.⁸ Because of the increasing interest of incorporation of molecules into microporous hosts, it is important to know the properties of the hosts in considerable detail. In this study, we have explored how the alignment of azobenzene into relatively large single crystals (100 μm) of aluminophosphate ($\text{AlPO}_4\text{-5}$) framework influences its spectroscopic and photochemical properties. Our choice of aluminophosphate framework was based on the fact that it is a relatively inert framework with channel diameters of 8 Å, which should allow for ready penetration of azobenzene into the matrix.

There are two previous papers dealing with azobenzene in microporous materials.^{9,10} In particular, the results of the photochemistry of azobenzene on ZSM-5 appear contradictory to each other.^{9,10} Corma and co-workers reported that in large

pore zeolite Y or zeolite β with strong Brønsted acidity, photolysis of *trans*-azobenzene led to cyclization forming benzo[*c*]cinnoline and benzidine.⁹ The photolysis proceeded through a *trans* to *cis* isomerization, and the zeolite acidity was essential for the cyclization reaction. However, no photochemical cyclization was observed in narrow pore zeolites such as ZSM-5, even in the presence of acidic functionalities. This was reasonably explained as arising because of the tight fit of the molecule in the <6 Å channels, which precluded isomerization of azobenzene. This lack of isomerization is consistent with previous studies of stilbene in ZSM-5, where enhanced fluorescence lifetimes were observed, along with lack of any photoisomerization.^{11,12} Caro and co-workers found that visible and ultraviolet radiation photolysis of azobenzene in ZSM-5 led to reversible *cis*–*trans* isomerization.¹⁰ The difference from stilbene photochemistry in ZSM-5 was rationalized based on the fact that two pathways for photoisomerization are available to azobenzene, an inversion and a rotation mechanism.⁴ The inversion requires a smaller volume, and it was proposed that this was the mechanism by which photoisomerization of azobenzene is occurring in ZSM-5. However, this would only hold for visible photolysis, since various studies in the literature indicate that the isomerization with ultraviolet light in resonance with the $\pi \rightarrow \pi^*$ band proceeds through a rotation mechanism.¹³ This would suggest that reversible photoisomerization of azobenzene in ZSM-5 should not be occurring. It was also reported by Caro and co-workers¹⁰ that photochemical *cis*–*trans* isomerization of azobenzene in $\text{AlPO}_4\text{-5}$ led to changes in refractive index of the crystals because of alignment changes of the enclosed azobenzene.

In this study, we have examined the spectroscopy and photochemistry of *trans*-azobenzene loaded into $\text{AlPO}_4\text{-5}$ and report that even though the $\text{AlPO}_4\text{-5}$ framework is not considered to be an acidic framework, the acid sites present lead to interactions between the $\text{AlPO}_4\text{-5}$ framework and azobenzene. This leads to observable fluorescence under ambient conditions as well as partial photocyclization of a fraction of the loaded

azobenzene and reversible cis–trans isomerization of the rest of the azobenzene. Thus, the photochemistry of azobenzene in a relatively “inert” microporous framework such as aluminophosphate $\text{AlPO}_4\text{-5}$ is considerably more complex than had been previously reported.

Experimental Section

Relatively large and uniform crystals of $\text{AlPO}_4\text{-5}$ were synthesized according to the procedure described by Finger and co-workers.¹⁴ The dispersed aluminum oxide hydrate sol was prepared by slowly adding 1.3889 g of boehmite to 40.0 mL of water in the presence of 0.8 mL of 1.4% HNO_3 and was stirred vigorously for 45 min. A solution containing 6.6 mL of 17% H_3PO_4 , 2.1 mL of triethylamine, and 10 mL of water was added dropwise to the aluminum oxide hydrate sol to form a gel. The gel was then transferred into Teflon-lined bomb reactors and heated at 463 K for 24 h without agitation. The large $\text{AlPO}_4\text{-5}$ crystals were formed hydrothermally under autogenous pressure. The $\text{AlPO}_4\text{-5}$ crystals were washed with Nanopure water and dried in air. The $\text{AlPO}_4\text{-5}$ was calcined at 923 K with flowing oxygen for 4 days and was activated at 673 K for 12 h under a dynamic vacuum prior to loading of azobenzene. The loading procedure involved heating a mixture of *trans*-azobenzene and $\text{AlPO}_4\text{-5}$ with a ratio of 1:10 by weight to 100 °C for 4 h in a reactor under static vacuum. The mixture was then Soxhlet extracted with methanol for 2 days to remove azobenzene from the surface of the loaded azobenzene/ $\text{AlPO}_4\text{-5}$ sample. All the extract solutions were collected and the amount of *trans*-azobenzene was determined by absorption spectroscopy. This allowed us to estimate the loading of azobenzene in $\text{AlPO}_4\text{-5}$ to be 5 wt %. The final loaded azobenzene/ $\text{AlPO}_4\text{-5}$ sample had an even light yellow color. Recovery of the organics in the $\text{AlPO}_4\text{-5}$ was done by dissolution of the framework by treatment with a 20% citric acid solution for 3 h. The resulting solution was neutralized with 1 M NaOH solution, and the organic material was extracted with hexane.

The scanning electron micrographs (SEM) were taken with a JEOL JSM-820. The $\text{AlPO}_4\text{-5}$ crystals for SEM were dispersed as a film on a metal stud and evacuated. It was then coated with gold/palladium to 150 Å thickness.

The UV–vis absorption and diffuse reflectance spectra were obtained with a Shimadzu spectrophotometer UV-265 with a Harrick diffuse reflection attachment. Fluorescence spectra were taken on a Spex Fluorolog-2 series F112 spectrofluorometer (Instruments S.A.) In the excitation part of the instrument, a 360 nm filter needed to be used after the single monochromator to minimize the background from the scattered light. The infrared spectra were taken on a Mattson Cygnus FTIR spectrometer with 4.0 cm^{-1} resolution. The sample chamber was purged with nitrogen to eliminate water and carbon dioxide. All spectroscopic data were analyzed with Grams/32 provided by Galactic Industries Corp.

The photolysis was carried out using the Spectra-Physics model 171 argon ion laser lasing at 476.5 nm wavelength and Coherent Innova 100 krypton ion laser lasing in broad-band UV, with primary intensity at two wavelengths of 350.7 and 356.4 nm. The azobenzene/ AlPO_4 sample (150 mg) was pressed into 13 mm pellets, evacuated at room temperature, and then transferred to an anaerobic cell covered with a quartz lid. Laser power at the cell surface was 100 mW and spread into a circular beam of diameter of 0.5 cm. The photolysis was carried out for 20 min at any one time.

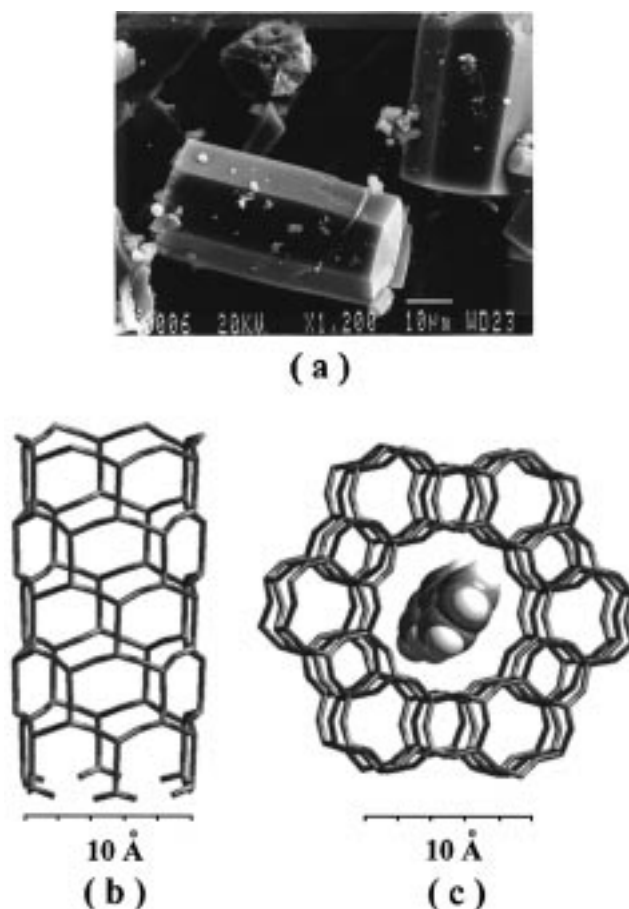


Figure 1. (a) SEM of $\text{AlPO}_4\text{-5}$ crystals. View of a channel of $\text{AlPO}_4\text{-5}$ (b) perpendicular and (c) along the “c” axis. The fit of *trans*-azobenzene within the 8 Å channel is also shown.

Results

A typical SEM picture of $\text{AlPO}_4\text{-5}$ used in this study is shown in Figure 1a along with a view of the structure along one of the channels (Figure 1b). Figure 1c shows a view of a *trans*-azobenzene molecule surrounded by the 8 Å twelve-ring channel, clearly demonstrating that azobenzene can penetrate along its long axis through the channel system of $\text{AlPO}_4\text{-5}$. The loading level of *trans*-azobenzene in the present study is of the order of 5 wt %. At these loading levels, we estimate that with uniform distribution, molecules of azobenzene are separated by about 7 Å.

Figure 2a shows the diffuse reflectance spectrum of *trans*-azobenzene loaded onto $\text{AlPO}_4\text{-5}$ and Figure 2b is that of the azobenzene in hexane obtained by extraction after dissolution of the $\text{AlPO}_4\text{-5}$ framework. It is clear that incorporation of *trans*-azobenzene into $\text{AlPO}_4\text{-5}$ is having a major influence on the electronic spectra, including red shift of the 313 nm band to 323 nm and considerable enhancement in intensity of a band at 418 nm.

Figure 3 shows the fluorescence of the azobenzene/ $\text{AlPO}_4\text{-5}$. Upon 360 nm excitation, the emission maximum is observed at 518 nm and tails out into the red. The extracted azobenzene/hexane showed no emission, as is expected from previous studies.¹⁵

Photolysis of azobenzene/ $\text{AlPO}_4\text{-5}$ under anaerobic conditions was followed by diffuse reflectance spectroscopy. The samples were photolyzed by laser excitation at ~350 and 476.5 nm for periods of 20 min, the time beyond which no more spectral changes were observed. Careful and accurate repositioning of

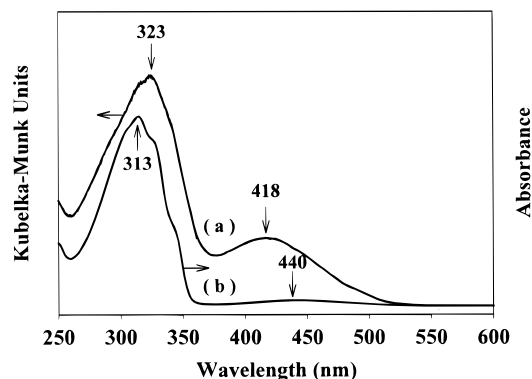


Figure 2. (a) Diffuse reflectance spectrum of azobenzene/ $\text{AlPO}_4\text{-5}$ and (b) UV-visible spectrum obtained by dissolution of the azobenzene/ $\text{AlPO}_4\text{-5}$ and extraction into hexane.

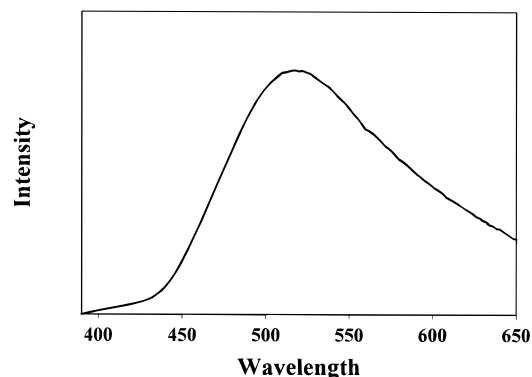


Figure 3. Emission spectrum of azobenzene/ $\text{AlPO}_4\text{-5}$ (excitation 360 nm).

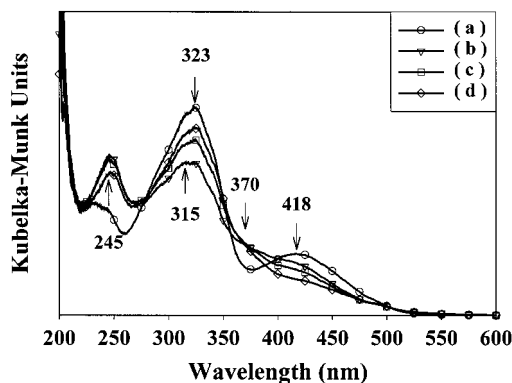


Figure 4. Diffuse reflectance spectra of (a) azobenzene/ $\text{AlPO}_4\text{-5}$ and after photolysis with (b) UV light (~ 350 nm), (c) visible light (476.5 nm), and (d) heated at 100 °C for 1 h.

sample in the diffuse reflectance instrument before and after photolysis was necessary to obtain reproducible spectra with peak intensities within a range of 10%. Figure 4 shows the spectral changes obtained during the following photolysis sequence: ultraviolet-visible-heat. The diffuse reflectance spectrum of the initial azobenzene/ $\text{AlPO}_4\text{-5}$ is shown in Figure 4a. After ultraviolet light exposure, new bands are observed around 245 and 315 nm along with increased intensity around 370 nm and a decrease in intensity of the 323 and 418 nm bands (Figure 4b). Visible light photolysis of the UV-photolyzed sample shows slight decreases in intensities of the 245 and 418 nm bands along with an increase in intensity of the 323 nm band (Figure 4c). Heating the sample after UV photolysis to 100 °C under vacuum for 1 h promotes the changes observed under visible excitation, i.e., decrease of the 245 and 418 nm bands and increase in intensity of the 323 nm band (Figure 4d).

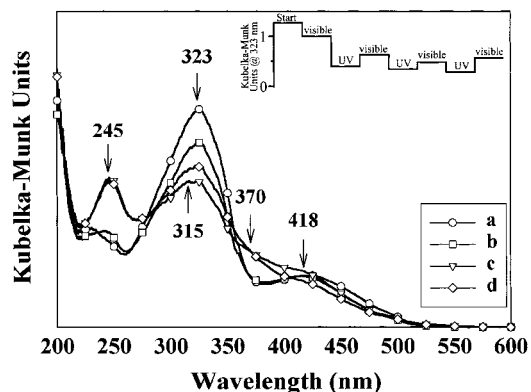


Figure 5. Diffuse reflectance spectra of (a) azobenzene/ $\text{AlPO}_4\text{-5}$ and after photolysis with (b) visible light (476.5 nm), (c) UV light (~ 350 nm), and (d) visible light (476.5 nm). The inset shows the intensity at 323 nm as a function of sequence of photolysis steps at visible and UV wavelengths.

It is important to note that sequence of photolysis and heating the sample does not restore the spectrum of the starting azobenzene/ $\text{AlPO}_4\text{-5}$ and that new absorption bands are being observed.

Figure 5 shows the diffuse reflectance spectra after a different sequence of photolysis: visible-ultraviolet-visible. Analysis of Figure 5 shows that visible photolysis of the initial azobenzene/ $\text{AlPO}_4\text{-5}$ sample (Figure 5a) results in a weak but distinct band at 245 nm, along with a decrease in the 323 nm band (Figure 5b). Photolysis with ultraviolet radiation results in significant increase of the 245 nm band and appearance of a band at 315 nm along with increased intensity at 370 nm and significant decrease of intensity at 323 nm (Figure 5c). The spectrum in this case resembles Figure 4b, obtained directly after ultraviolet photolysis of the azobenzene/ $\text{AlPO}_4\text{-5}$ sample. After the sample has been exposed to ultraviolet radiation, it reaches a state from which reversible spectral changes as a function of visible and ultraviolet photolysis can be observed, though under no conditions is the original spectrum of the starting azobenzene/ $\text{AlPO}_4\text{-5}$ recovered. Figure 5d shows the spectrum after visible light photolysis. We repeated the sequence of visible-ultraviolet photolysis several times, and the inset in Figure 5 demonstrates how the intensity at the wavelength of 323 nm varies during such a sequence. It shows that there is a significant decrease in intensity at 323 nm upon initial UV photolysis, after which a reversible trend of the intensity as a function of UV-visible photolysis is observed. The fact that the intensity of the 323 nm band does not exactly recover to the steady-state values on repeated runs is because of problems with positioning the sample at exactly the same spot in the diffuse reflectance spectrometer after photolysis. Intensity around 420 nm exhibited the trend opposite to that observed at 323 nm.

A sample of azobenzene/ $\text{AlPO}_4\text{-5}$ that was photolyzed by ultraviolet light at ~ 350 nm was treated with citric acid to dissolve the aluminophosphate framework, and the organics extracted into hexane. The extract after evaporation was examined by infrared spectroscopy, and the spectrum is shown in Figure 6a. Several of the bands are due to *trans*-azobenzene (Figure 6b), which is not surprising considering that the surface of the azobenzene/ $\text{AlPO}_4\text{-5}$ pellet was photolyzed and the light did not penetrate through the whole pellet. Figure 6c shows the spectrum remaining behind from Figure 6a after the bands due to *trans*-azobenzene (Figure 6b) were subtracted out using the *trans*-azobenzene band at 773 cm^{-1} as the normalizing peak. Almost all the bands in this difference spectrum can be assigned

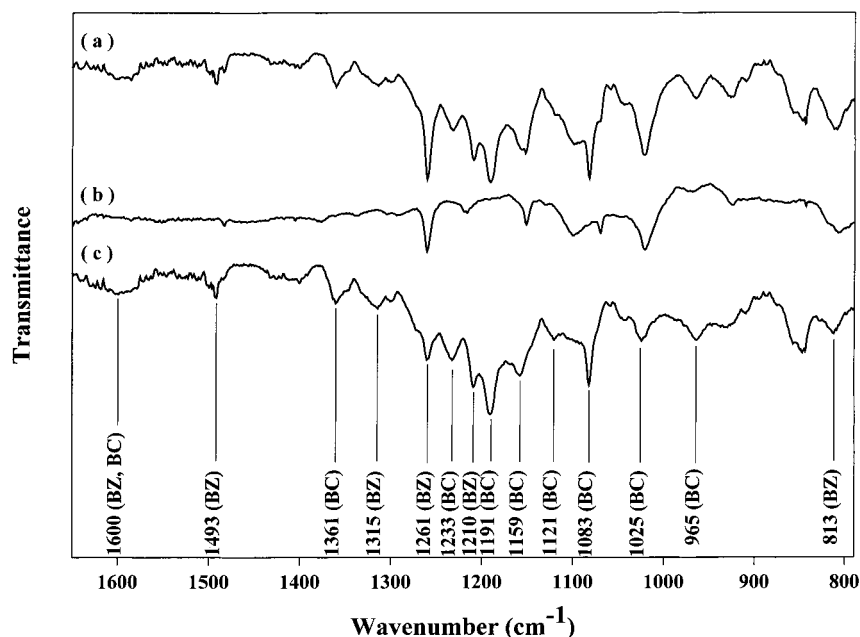


Figure 6. Infrared spectra of extract obtained by dissolution of the azobenzene/ $\text{AlPO}_4\text{-5}$ (a) after UV (~ 350 nm) photolysis and (b) as synthesized sample prior to photolysis. (c) Difference spectrum between spectra a and b obtained by subtracting out the *trans*-azobenzene contribution (773 cm^{-1} band of *trans*-azobenzene was used as the peak whose intensity was completely removed from spectrum a). BC = benzo[*c*]cinnoline, BZ = benzidine.

to benzo[*c*]cinnoline and benzidine, based on literature reports on the infrared spectra of these two compounds.^{9,16–18} As has been shown previously,⁹ the extraction of entrapped species by dissolution of the framework is not quantitative. Thus, the infrared shown in Figure 6c is a definite indication that benzidine and benzo[*c*]cinnoline are formed upon photolysis, though information about their relative ratios cannot be deduced from the spectrum.

Discussion

Interaction of Azobenzene with the $\text{AlPO}_4\text{-5}$. *Acidity of the $\text{AlPO}_4\text{-5}$ Framework.* The framework of $\text{AlPO}_4\text{-5}$ has an Al/P ratio of 1 and thus there is strict alternation of Al and P atoms at tetrahedral nodes, with the structure being electrically neutral.¹⁹ Both the absorption and emission spectra of *trans*-azobenzene are considerably altered upon incorporation into $\text{AlPO}_4\text{-5}$ (Figures 2 and 3). Since there are no extra framework cations in $\text{AlPO}_4\text{-5}$, these changes must arise because of interactions of azobenzene with the aluminophosphate framework. Several papers have reported on the types of acidity present in $\text{AlPO}_4\text{-5}$ framework.^{20–22} The probes for measuring acidity include pyrrole adsorption, temperature-programmed desorption of ammonia, and pyridine and cumene cracking reactions. These studies indicate that compared to conventional aluminosilicate zeolites or even silicoaluminophosphate framework, the acidity of $\text{AlPO}_4\text{-5}$ is relatively weak, though clearly present. There is evidence for both Brönsted and Lewis acid sites, with the amount of Lewis acid sites increasing proportionately with temperature of activation. The Brönsted acidity arises from OH groups (Al–OH and P–OH) present on the surface of the crystals as well as at defect sites.²² The Lewis acids arise from low-coordinated Al atoms on the lattice.²² Possible interactions of azobenzene with framework acidic groups would involve donation of the nitrogen lone pairs on the azo group to the Lewis acids or protonation of the nitrogen.

Electronic Spectral Changes. The electronic spectrum of *trans*-azobenzene in solution is characterized by a strong band at 313 nm and a very weak band at 440 nm, as seen in Figure

2b, which is the spectrum of azobenzene (in hexane) obtained by dissolution of the azobenzene/ $\text{AlPO}_4\text{-5}$ sample. The appearance of a new band at 418 nm and the red shifting of the 313 nm band must be from azobenzene– $\text{AlPO}_4\text{-5}$ interactions, and is not arising from the incorporation procedure. It is known that if the azo nitrogens of *trans*-azobenzene are protonated, then a strong absorption band arises at 425 nm, which is primarily $\pi \rightarrow \pi^*$ in nature.^{23,24} For *trans*-azobenzene, the band observed at 440 nm is weak in intensity and primarily $n \rightarrow \pi^*$ in nature.³ Complexation of the nitrogen lone pairs also leads to considerable decrease in intensity of the 315 nm band.²⁴ We propose that only a fraction of the *trans*-azobenzene molecules in the $\text{AlPO}_4\text{-5}$ are involved in acid–base reactions with the framework. Figure 7a shows that approach of the *trans*-azobenzene to the Al atoms on the framework is severely limited because of the arrangement of the benzene rings. We estimate a distance of 4.5 Å as the closest approach. Thus, for *trans*-azobenzene, it is unlikely that interactions with the Lewis acid sites are occurring, which suggests that protonation of the azo nitrogen by Brönsted acid sites is the only possibility. Also, since the number of acid sites in $\text{AlPO}_4\text{-5}$ is limited, only a fraction of the *trans*-azobenzene molecules are protonated and contribute intensity to the 418 nm band. The rest of the *trans*-azobenzene molecules are not interacting with the framework and contribute primarily to the $\pi \rightarrow \pi^*$ band at 323 nm. Red shifting of the $\pi \rightarrow \pi^*$ band upon incorporation is indicative of a highly polar local environment. Even though the $\text{AlPO}_4\text{-5}$ framework has neutral charge, the local electronegativity difference between Al and P may give rise to a polar environment.²²

It is well known that azobenzene does not show fluorescence (even at 77 K) in powdered form, dissolved in solvents, or supported on solids.¹⁵ Thus, the emission from azobenzene in $\text{AlPO}_4\text{-5}$ also indicates interaction of azobenzene with the framework. Rau has reported that protonated azobenzene will exhibit fluorescence around 510 nm at 77 K.²⁴ This emission is only possible with azobenzene if the lone pair electrons are bonded, resulting in the lowest excited state being $^1(\pi\pi^*)$. The

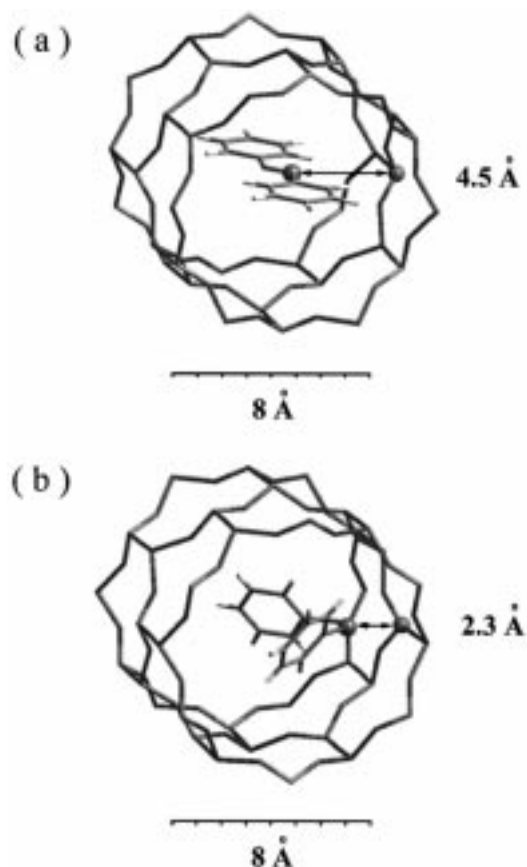


Figure 7. Closest approach of (a) *trans*-azobenzene and (b) *cis*-azobenzene to a tetrahedral atom site of the $\text{AlPO}_4\text{-5}$ framework.

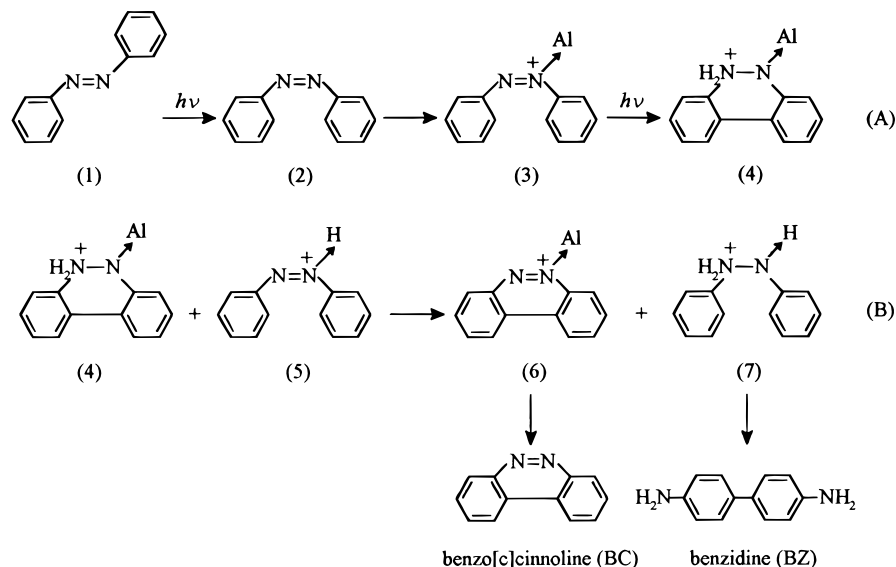
low temperature is necessary to restrict the floppiness of the molecules. Thus, in $\text{AlPO}_4\text{-5}$, the emission is being caused by the same population of protonated azobenzene molecules that contribute to the absorption band at 418 nm. The fact that fluorescence is observed at room temperature indicates that the $\text{AlPO}_4\text{-5}$ channels restricts the floppiness of the azobenzene molecules. The only other report of room temperature fluorescence around 510 nm is from azobenzene at the fluorocarbon–water interface in a swollen Nafion– H^+ membrane.²⁵

Photolysis Chemistry. Photocyclization. The photolysis was done in an anaerobic environment to avoid any photooxi-

dation reactions. Diffuse reflectance spectra show that upon UV photolysis of the azobenzene/ $\text{AlPO}_4\text{-5}$, there appear new bands at 245, 315, and 370 nm, along with decrease in intensity of the bands of azobenzene (323, 418 nm). The reversible *cis*–*trans* photoisomerization of azobenzene has been extensively studied.¹ Typically, photolysis of *trans*-azobenzene in the UV (350 nm) leads to a photostationary state that is predominantly *cis*-azobenzene and is characterized by absorption bands at 250, 280 (shoulder), and 430 nm.¹ The additional spectral features (315, 370 nm) that are arising after photolysis of azobenzene/ $\text{AlPO}_4\text{-5}$ indicate formation of other species. The infrared spectra in Figure 6 convincingly demonstrate that after photolysis with ultraviolet light and extraction, benzo[*c*]cinnoline and benzidine are being formed. Electronic spectral changes also support the formation of these species. The benzinidinium cation absorbs at 252 nm, benzo[*c*]cinnoline has absorption bands at 250 and 315 nm, and upon protonation of one of the nitrogens, the long wavelength band shifts to 370 nm.^{23,25} Thus, the new bands observed after UV photolysis (Figure 5b) at 245, 315, and 370 nm can be assigned to benzo[*c*]cinnoline and benzidine. The formation of these species is only possible via photocyclization reactions, which are known to proceed efficiently in strongly protonic environments, such as 98% H_2SO_4 .^{3,23,26} Similar photocyclization chemistry has also been reported in highly acidic water swollen Nafion– H^+ membranes²⁴ and in protonic aluminosilicate zeolites,⁹ with complete conversion to benzidine and benzo[*c*]cinnoline. However, considering that the Brönsted site density in $\text{AlPO}_4\text{-5}$ is small, it is not the protons alone that are playing the major role in cyclization. Around the same time that the classic study of photocyclization of azobenzene in strong protonic acids was reported,^{23,26} it was also reported that photocyclization can occur in the presence of Lewis acid sites, such as FeCl_3 in the presence of the weak acid acetic acid.²⁷ This environment is more typical of what is present in $\text{AlPO}_4\text{-5}$, i.e., Lewis acids along with weak Brönsted acid sites.

On the basis of the accepted mechanism of photocyclization,^{3,23,27} the interaction of the photochemically generated *cis*-azobenzene with acid sites in the $\text{AlPO}_4\text{-5}$ is necessary. It is important to note that as compared to the *trans* form, the geometry of the *cis*-azobenzene promotes unrestricted approach of the azo group to the walls of the $\text{AlPO}_4\text{-5}$, the sites for Lewis acidity. The contrast in the approach between the two isomers

SCHEME 1



toward the acid sites on the framework is shown in Figure 7. Scheme 1 explains the results.

After *trans* (**1**) to *cis* (**2**) conversion, the *cis*-azobenzene can interact readily with the Lewis acid sites on the framework forming **3**. Upon further photolysis these complexed *cis* isomers cyclize along with prototopic shifts to form **4**. Reaction with protonated azobenzenes (**5**) then leads to benzo[*c*]cinnoline and benzidine.

Photoisomerization. After the initial UV photolysis of azobenzene/AlPO₄-5 and formation of benzidine and benzo[*c*]cinnoline, a state is reached from which reversible spectral changes are observed if visible light (476.5 nm) follows ultraviolet (~350 nm) photolysis (e.g., Figure 5c,d). There is a slight decrease in intensity of the 245 nm band, growth in intensity of the 323 nm band, as well as decrease in intensity of the broad band around 420 nm, indicative of a *cis* → *trans* transformation. Figure 5 (inset) shows the plot of the intensity at 323 nm (due to the *trans* isomer) upon several cycles of visible and ultraviolet photolysis and shows that the intensity increase and decrease is reversible. Monitoring the intensity around 420 nm (due to the *cis* isomer) showed the opposite trend. Thus, visible light promotes the *cis* to *trans* conversion and the reverse for ultraviolet light, in both cases reaching a photostationary state. Molecular modeling studies indicate that there is enough room in the 8 Å channels of AlPO₄-5 to accommodate the transition states required for either the rotation or inversion mechanism. The *cis*-azobenzene is also known to convert to the *trans* form thermally.^{1,3} We observe an increase in intensity of the 323 nm band due to the *trans* form and a decrease in intensity of the 245 nm band due to the *cis* form because of the thermal conversion of *cis* to *trans* (Figure 4d). It is also important to note in Figure 4d that after photolysis and heat treatment, the intensity of the *n* → π^* transition around 400–440 nm is beginning to resemble *trans*-azobenzene in solution (Figure 2b). This is not surprising because the *trans*-azobenzene–framework acid interactions that were giving rise to enhanced intensity in the 418 nm region are no longer present, being replaced by the benzo[*c*]cinnoline– and benzidine–framework acid interactions.

The degree to which photocyclization occurs is determined by the number density of acid sites in AlPO₄-5. Corma et al.⁹ also noted that in zeolite Y, the yield of benzo[*c*]cinnoline, which is a measure of the photocyclization reaction, decreased as the number of acid sites present in the framework was decreased by substitution of Al by Si. Thus in AlPO₄-5, once the photocyclization reaction is complete because all the acid sites are occupied, the rest of the azobenzene molecules that have weak interactions with the aluminophosphate framework exhibit the conventional *cis*–*trans* photoisomerization chemistry.

Conclusions

Aluminophosphate frameworks are not regarded as acidic because of their inability to catalyze hydrocarbon transformations. However, they do contain Lewis and Brønsted acid sites. This study has focused on the aluminophosphate AlPO₄-5, which

can be synthesized as reasonably large 100 μ m crystallites. Their 8 Å channels can readily accommodate *trans*-azobenzene. Significant spectral perturbations of the azobenzene chromophore are found upon incorporation into AlPO₄-5. These include enhanced intensity of a band at 418 nm in the absorption spectrum and room temperature fluorescence at 518 nm. This is explained as occurring due to protonation of the azo group by Brønsted acid sites of AlPO₄-5. Upon photolysis, the *trans*-azobenzene isomerizes to the *cis* form, which can then interact with the Lewis acid sites of the framework. Further photolysis leads to photocyclization, resulting in formation of benzo[*c*]cinnoline and benzidine, and parallels the solution-based chemistry reported with Lewis acids such as FeCl₃. However, because the number density of acid sites in AlPO₄-5 is low, only a fraction of the azobenzene molecules undergo photocyclization. Reversible *cis*–*trans* photoisomerizations modulated by ultraviolet and visible radiation are observed for the rest of the azobenzene molecules.

Acknowledgment. We acknowledge funding by the Department of Energy, Basic Energy Sciences Division.

References and Notes

- (1) Rau, H. *Photochemistry and Photophysics*; Rabek, J. F., Ed.; CRC Press: Boca Raton, Florida, 1990; Vol. 2, pp 119–141.
- (2) Zollinger, H. *Colour Chemistry, Synthesis, Properties and Applications of Organic Dyes*; VCH: Weinheim, 1987.
- (3) Griffiths, J. *Chem. Soc. Rev.* **1972**, 1, 481.
- (4) Monti, S.; Orlandi, G.; Palmieri, P. *Chem. Phys.* **1982**, 71, 87.
- (5) Kumar, S. J.; Neckers, D. C. *Chem. Rev.* **1989**, 89, 1915.
- (6) Shimomura, M.; Kunitake, T. *J. Am. Chem. Soc.* **1987**, 109, 5175.
- (7) (a) Ramamurthy, V.; Eaton, D. F. *Chem. Mater.* **1994**, 6, 1128. (b) Herron, N. *J. Inclusion Phenom. Mol. Recognit. Chem.* **1995**, 21, 283.
- (8) Gfeller, N.; Magelski, S.; Calzaferri, G. *J. Phys. Chem. B* **1998**, 102, 2433.
- (9) Corma, A.; Garcia, H.; Ibarra, S.; Marti, V.; Miranda, M. A.; Primo, J. *J. Am. Chem. Soc.* **1993**, 115, 2177.
- (10) Hoffman, K.; Marlow, F.; Caro, J. *Adv. Mater.* **1997**, 9, 575.
- (11) Gessner, F.; Olea, A.; Lobaugh, J. H.; Johnston, L. J.; Scaiano, J. C. *J. Org. Chem.* **1989**, 54, 259.
- (12) Ramamurthy, V.; Caspar, J. V.; Corbin, D. R. *J. Am. Chem. Soc.* **1991**, 113, 594.
- (13) Rau, H. *J. Photochem.* **1984**, 26, 221.
- (14) Finger, G.; Richter-Mendau, J.; Bülow, M.; Kornatowski, J. *Zeolites* **1991**, 1, 443.
- (15) Rau, J. *Ber. Bunsen-Ges. Phys. Chem.* **1971**, 75, 1343.
- (16) Neto, H.; Nocentini, M.; Muniz-Miranda, M.; Sbrana, G. *J. Mol. Struct.* **1990**, 218, 423.
- (17) Rahman, S. M. F.; Ahmad, J.; Haq, M. M. *J. Inorg. Nucl. Chem.* **1972**, 34, 1460.
- (18) Ohmasa, M.; Kinoshita, M.; Akamatu, H. *Bull. Chem. Soc. Jpn.* **1971**, 44, 395.
- (19) Bennett, J. M.; Dytrych, W. J.; Pluth, J. J.; Richardson, J. W., Jr.; Smith, J. V. *Zeolites* **1986**, 6, 349.
- (20) Akolekar, D. B. *Zeolites* **1994**, 14, 53.
- (21) Akolekar, D. B.; Huang, M.; Kaliaguine, S. *Zeolites* **1994**, 14, 519.
- (22) Hedge, S. G.; Ratnasamy, P.; Kustov, L. M.; Kazansky, V. B. *Zeolites* **1988**, 8, 137.
- (23) Badger, G. M.; Drewer, R. J.; Lewis, G. E. *Aust. J. Chem.* **1966**, 19, 643.
- (24) Rau, H. *Ber. Bunsen-Ges. Phys. Chem.* **1967**, 71, 48.
- (25) Tung, C.-H.; Guan, J.-Q. *J. Org. Chem.* **1996**, 61, 9417.
- (26) Lewis, G. E. *Tetrahedron Lett.* **1960**, 9, 12.
- (27) Hugelshofer, P.; Kalvoda, J.; Schaffner, K. *Helv. Chim. Acta* **1960**, 43, 1322.